Centralized Power Allocation for Interference Limited Networks

Cédric Abgrall[†‡], Emilio Calvanese Strinati[†] and Jean-Claude Belfiore[‡]
Email: cedric.abgrall@cea.fr, emilio.calvanese-strinati@cea.fr and jean-claude.belfiore@telecom-paristech.fr

[†]CEA, LETI, MINATEC
17, rue des Martyrs - 38054 Grenoble, France

[‡]TELECOM ParisTech
46, rue Barrault - 75013 Paris, France

ABSTRACT

***Abstract*—The goal of our work is to limit in-band inter-cell interference in wireless communication cellular systems. Based on interference classification techniques, we propose a novel centralized inter-cell power allocation algorithm which computes the minimum power budget required in each cell to meet its local quality of service (QoS) constraints. Both analytical and numerical results applied to cellular networks show how our algorithm permits to notably reduce both power budget and harmful effects of in-band inter-cell interference, while meeting QoS constraints of users in each cell.**

***Index Terms*—Interference limited network, resource management, power allocation, interference mitigation.**

I. INTRODUCTION

Future wireless communication systems target high capacity transmissions in interference limited scenarios. Furthermore, network operators have to guarantee minimal QoS requirements to a growing number of consumers. The interference issue becomes a prejudicial bottleneck in cellular networks.

Several methods have been proposed to limit the detrimental effects of interference experienced by destinations; main techniques are introduced hereinafter. First, resource allocation management can avoid in-band concurrent transmissions to cause intra-cell and inter-cell interference by full time and frequency orthogonalization of resources. But such orthogonal allocations are not spectral efficient. More flexible approaches are promising [1]: Frequency Reuse for instance consists in reallocating part of frequency resources in adjacent spatial locations. Second, signal processing techniques can help in coping with interference: Dirty Paper Coding, Successive Interference Cancellation (SIC), Sphere Decoder and challenging Interference Alignment (IA) [2]–[6]. IA technique processes a specific filtering at transmission and reception to align signal and interference on two different eigenspaces, each with a part of the available amount of degrees of freedom. Interference-free transmissions are reached by sacrificing some degrees of freedom. Third, channel aware adaptive mechanisms such as Adaptive Modulation Coding, Graph Colouring, Convex Optimization and Power Control can also limit the interference issue [7]–[9]. A well-known approach is Water-Filling where a cost function is optimized under constraints [10].

In the literature, theoretical surveys on performance of wireless communications in interference limited networks proposed a classification of perceived interference in five regimes of interference, namely *noisy*, *weak*, *moderately weak*, *strong* and *very strong* [11][12]. Han and Kobayashi proposed in [13] to decompose, at the coder, messages into a *private* part for an exclusive destination and a *common* part decodable by all destinations. The proportion of private and common information in the global message can be matched up with the interference classification: messages are entirely *private* in the *noisy* regime, while they are entirely *common* in the *very strong* regime. Superposition coding lets combine both kinds of messages. Nevertheless, such a five-level classification requires complex processing which can be met theoretically but not in practice.

In this paper, an adaptive low-complexity interference classifier is first proposed, then exploited in a centralized power allocation algorithm for multi rate-constrained interfering cells. A common network controller computes, according to the momentary communication context, the minimal transmission power vector which lets to meet all QoS constraints.

II. NOTATIONS AND SYSTEM MODEL

In our work, we consider a system with two neighbour cells, $\mathscr{C}_1$ and $\mathscr{C}_2$, whose downlink transmissions occur over a common communication band. Each cell $\mathscr{C}_i$ consists of a base station (source s_i) and a single user equipment (destination d_i); both are single-antenna. d_i is able to decode the interfering message x_j sent by s_j, even if the information message x_i from s_i is the one dedicated to him. Communication rates are limited by inter-cell interference and Gaussian noise $z_i \sim \mathscr{N}(0, N_0)$. The received signal at d_i is given by

$$y_i = g_{i,i} \cdot x_i + g_{j,i} \cdot x_j + z_i$$

where the channel gain $g_{j,i}$ between s_j and d_i is assumed constant during at least one frame transmission. Our system is modelled as the Interference Channel (IC) [13] illustrated on Figure 1a. Cells are rate and power constrained, *i.e.,* s_i must ensure at least the target information rate $\mathbf{R_i}$ for its destination d_i and s_i cannot transmit with a power P_i exceeding the system constraint $\mathbf{P_{i,max}}$.

Focusing on destination viewpoint, our system can be divided into two many-to-one IC denoted by $(\Delta_i)_{i=1,2}$. Subsystem Δ_i accounts for the whole cell $\mathscr{C}_i$ with its interfering neighbour source s_j. Δ_1 is illustrated on Figure 1b and seems to be the well-known two-user Multiple Access Channel (MAC) [14]. Nevertheless, Δ_i differs from a two-user

978-1-4244-3574-6/10/$25.00 ©2010 IEEE

MAC. Indeed, with a MAC both sources send intentionally information to the common destination, whereas with Δ_i crossed channels $g_{j,i}$ convey interference instead of information. Furthermore, a MAC tries to optimize rates pair $(R_1; R_2)$, whereas Δ_i cannot control crossed-rate R_j and has to deal with R_j without reducing R_i. So as to insist on these fundamental differences between a MAC and Δ_i, we refer for Δ_i to information and crossed rate respectively as ρ_i and μ_i instead of R_i and R_j. But we have $\mu_i = \rho_j = R_j$ in practice.

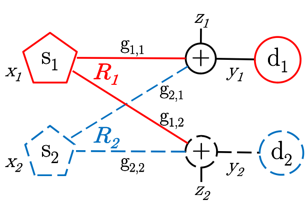

(a) Two-user Interference Channel

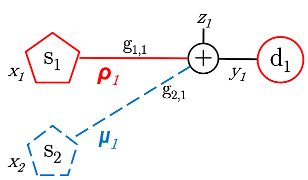

(b) Δ_1: Many-to-one IC

Fig. 1: Adopted system models for $\mathscr{C}_1$ and $\mathscr{C}_2$

Finally, variables A_i, B_i, C_i and A used hereafter are introduced, while γ_i and δ_i respectively denote SNR and INR perceived at destination d_i.

$$\gamma_i = \frac{g_{i,i} \cdot P_i}{N_0} \tag{1}$$

$$\delta_i = \frac{g_{j,i} \cdot P_j}{N_0} = f_j \cdot \gamma_j, \quad \text{with } f_j = \frac{g_{j,i}}{g_{j,j}} \tag{2}$$

$$A_i = 2^{\rho_i} - 1, \quad B_i = 2^{\mu_i} - 1 = A_j \tag{3}$$

$$C_i = 2^{\rho_i + \mu_i} - 1 = (A_i + 1)(B_i + 1) - 1 = A \tag{4}$$

III. Simplified Interference Classification

In this section we derive an interference classifier which can be performed with low complexity at a centralized network controller (NC) devoted to power allocation. Since *private* and *common* data flows [13] cannot be superposed in practical coders, we force the sources to output a single *common* flow. To this end, we assumed the destinations can decode interfering messages. However, the decoding process at destination d_i is adapted to the perceived INR δ_i: the decoder treats interfering message x_j either as a *private* or as a *common* message. We classify interference into three regimes. Either, the interference signal is 'weak' (roughly at noise level) (see III-A). In this case we process interference as additional noise. Otherwise, we decode interference, either before processing the intended signal (see III-B.1), or jointly with the intended signal (see III-B.2). Classification of perceived interference is done by NC and then fed back to d_i which can so adopt effective interference processing strategies. The overall process is ensured by NC, coders are not requested to do specific tasks.

Performance of MAC and IC is typically evaluated by their capacity region, which is the set of all simultaneously achievable rate pairs $(R_1; R_2)$, *i.e.,* rates that can be transmitted with arbitrarily small error probability. Capacity region upper bounds have been proposed for MAC and IC [11]–[15]; some of these bounds are used below to introduce our interference classifier for Δ_i.

A. "Noisy" Interference Regime

The "noisy" regime corresponds to the most conventional way for dealing with interference, *i.e.,* treating interference signal as additional thermal noise. Applicability of such an approach is directly related to the capacity of d_i to decode (or not) the interfering message x_j. If the perceived interfering signal is too weak to be decoded, then processing x_j as additional noise is optimal.

Equation (5) specifies the region where this regime is applicable, while equation (6) exhibits an upper bound for the achievable information rate ρ_i. Performance can be expressed either in terms of rates with ρ_i and μ_i, or in terms of SNR with γ_i and $\gamma_j = \frac{1}{f_j} \cdot \delta_i$.

$$\mu_i \geq \log_2 (1 + \delta_i) \quad \Leftrightarrow \quad f_j \cdot \gamma_j \leq B_i \tag{5}$$

$$\rho_i \leq \log_2 \left(1 + \frac{\gamma_i}{1 + f_j \cdot \gamma_j}\right) \quad \Leftrightarrow \quad \gamma_i \geq A_i (1 + f_j \cdot \gamma_j) \tag{6}$$

B. "MAC-like" Interference Regimes

Contrary to the "noisy" regime, interfering signal is sensed here with a power sufficiently high to be exploited: decoding it rather than processing it as noise is more judicious. Consequently, both messages are decoded, as a two-user MAC would make it ("MAC-like"). The achievable capacity region of the two-user MAC can thus be exploited to evaluate our performance. This region is bounded by individual rates of both sources and by the sum of these rates (sum-rate):

$$\begin{cases} R_1 \leq \log_2 (1 + \gamma_1) \\ R_2 \leq \log_2 (1 + \gamma_2) \\ R_1 + R_2 \leq \log_2 (1 + \gamma_1 + \gamma_2) \end{cases} \tag{7}$$

The capacity region of Δ_i can be derived from (7) as:

$$\begin{cases} \rho_i \leq \log_2 (1 + \gamma_i) \\ \mu_i \leq \log_2 (1 + \delta_i) \\ \rho_i + \mu_i \leq \log_2 (1 + \gamma_i + \delta_i) \end{cases} \tag{8}$$

The second inequality in (8) does not hold since the crossed-link conveys interference instead of information; there is thus no reason for Δ_i to limit its performance to the achievable rate on this interfering link. So, only two regimes are really relevant; their performance is derived hereafter.

B.1) "Interference Cancellation" Regime: Here, interference is so strong that it causes no degradation in comparison to a scenario without interference. Such an approach is known in literature as the *very strong* interference regime [16]. Optimal scheme consists in first decoding interfering signal while processing information signal as noise, then subtracting interference to the received signal and eventually, decoding the information signal cleaned from interference. Interference is then cancelled out. Equation (9) specifies the applicability range of this regime for Δ_i while (10) bounds the achievable information rate ρ_i and SNR γ_i. Referring to (7), this regime stands for the first inequality.

$$\mu_i \leq \log_2 \left(1 + \frac{\delta_i}{1 + \gamma_i}\right) \quad \Leftrightarrow \quad f_j \cdot \gamma_j \geq B_i (1 + \gamma_i) \tag{9}$$

$$\rho_i \leq \log_2 (1 + \gamma_i) \quad \Leftrightarrow \quad \gamma_i \geq A_i \tag{10}$$

B.2) "Jointly Decoding" Regime: With this regime, perceived interference is not strong enough to be decoded alone and not weak enough to be processed as noise; destination should jointly decode information and interference for recovering information data. This regime is jammed between bounds (5) and (9) of "noisy" and "interference cancellation" regimes:

$$\begin{aligned} & \log_2\left(1+\frac{\delta_i}{1+\gamma_i}\right) \leq \mu_i \leq \log_2\left(1+\delta_j\right) \\ \Leftrightarrow \quad & \frac{f_j \cdot \gamma_j}{1+\gamma_i} \leq B_i \leq f_j \cdot \gamma_j \end{aligned} \tag{11}$$

Achievable ρ_i and γ_i are derived from the third line of (8):

$$\rho_i \leq \log_2\left(1+\gamma_i+f_j \cdot \gamma_j\right)-\mu_j \quad \Leftrightarrow \quad \gamma_i \geq C_i-f_j \cdot \gamma_j \tag{12}$$

C. Achievable SNR Region for $\mathscr{C}_i$

Performance of our three-level interference classifier is illustrated hereafter for Δ_i. Since in practice $\mu_i = \rho_j = R_j$ holds (ρ_i and μ_i were just introduced for sake of clarity), variables B_i and C_i are useless (see (3) and (4)). Furthermore, each regime is completely defined by the knowledge of $(\gamma_i;\delta_i)$ and $(\mathbf{R_1};\mathbf{R_2})$ (see (5)–(12)). Therefore, parameters set $\mathscr{P}_S = \{\mathbf{R_1};\mathbf{R_2};f_1;f_2\}$ states performance for $\mathscr{C}_1$ and $\mathscr{C}_2$.

Usually, the region $(R_1;R_2)$ is used to derive achievable capacity region when rates are maximized for given powers. Since we seek to minimize allocated transmission power while meeting rates $(\mathbf{R_1},\mathbf{R_2})$, it suits better to derive the achievable power region. P_i is easily deduced from γ_i with (1). So we rather work in region $(\gamma_i;\delta_i)$ $(\delta_i = f_j \cdot \gamma_j)$ within which we derive the achievable SNR region $\mathscr{R}_i^*$, *i.e.,* the set of all pairs $(\gamma_i;\delta_i)$ that let Δ_i (or equivalently, $\mathscr{C}_i$) meet its target rate $\mathbf{R_i}$. $\mathscr{R}_i^*$ is shown on Figure 2, where $\gamma_{i,max}$ and $\delta_{i,max}$ state limitations $\mathbf{P_{i,max}}$ and $\mathbf{P_{j,max}}$. Dash-dot red lines illustrate the applicability boundaries (5) and (9) of the three regimes. Solid blue lines $(\mathscr{D}_i^k)_{k=1..3}$ show the lower bounds (6), (12) and (10) of $\mathscr{R}_i^*$, respectively for the "noisy", "joint decoding" and "interference cancellation" regimes. The blended shades of blue specify that $\mathscr{R}_i^*$ is located above blue lines $(\mathscr{D}_i^k)_k$. Figure 2 is obtained for a given communication scenario $\mathscr{P}_S$; changing one parameter in $\mathscr{P}_S$ impacts lines equations.

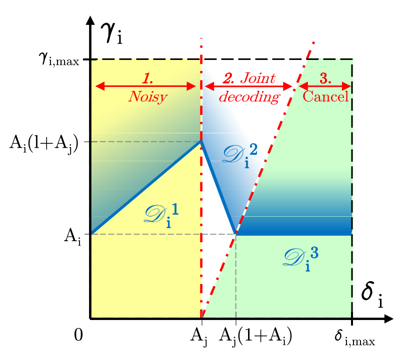

Fig. 2: Achievable SNR region $\mathscr{R}_i^*$ for cell $\mathscr{C}_i$

IV. Centralized Power Allocation Algorithm

In this section we develop our two-user centralized power allocation algorithm specifically designed to limit the undesired effects of in-band inter-cell interference. Each cell $\mathscr{C}_i$ targets to meet the transmission rate $\mathbf{R_i}$ with the lowest power P_i^* which cannot exceed $\mathbf{P_{i,max}}$. But power allocation is a Game Theory problem; s_i cannot set selfishly P_i^*: if s_i increases P_i for helping d_i, then $\mathscr{C}_i$ affects $\mathscr{C}_j$ which will react by increasing P_j, and so on until P_i and P_j will exceed power limitations.

With our approach, interference classification and power allocation for both cells are jointly performed by the centralized NC, prior to transmission. The goal of our algorithm is threefold. First, NC assigns power to jointly meet both rate requirements. Second, NC outputs the minimal transmission power vector $P^* = (P_1^*;P_2^*)$: any power lower than P^* does not meet rate requirements. Third, NC notifies destinations of their interference regime; efficient interference mitigation schemes can the be performed. Noise and full channel knowledge can be reached at NC by pilots or backhauling, whereas sources can broadcast target rates and power constraints. The main steps of our algorithm are developed below:

Step 1. s_i broadcasts $\mathbf{R_i}$ and $\mathbf{P_{i,max}}$ to NC.
Step 2. d_i estimates and broadcasts to NC γ_i and δ_i.
Step 3. NC estimates noise variance N_0.
Step 4. NC computes $\mathscr{R}_1^*$ and $\mathscr{R}_2^*$ with (6), (10) and (12).
Step 5. NC computes $\Gamma^* = (D_1^k)_k \cap (D_2^k)_k$; the pair O^* of optimal regimes is deduced from Γ^* (see Section V).
Step 6. NC deduces P^* from Γ^* and compares P^* to P_{max}.
Step 7. If $P^* > P_{max}$, then Time Sharing is performed.
Step 8. NC specifies P_i^* to s_i and O_i^* to d_i.

V. Optimal Solutions: Proof of Existence

Subsection III-C and on Figure 2 gave main performance results of our three-level classifier for subsystem Δ_i with a single destination. But our system counts two cells which interact because of in-band inter-cell interference. We prove here that there is always a finite and non-zero number of theoretical solutions for our problem of power allocation under rate-constraints.

It seems natural to superpose on the same figure both achievable SNR regions $\mathscr{R}_1^*$ and $\mathscr{R}_2^*$; Figure 2 is thus turned into Figure 3a. Lower bounds $(\mathscr{D}_1^k)_k$ and $(\mathscr{D}_2^k)_k$ are illustrated respectively by purple dashed lines and blue solid lines, while regimes applicability regions are delimited by dotted green lines for $\mathscr{C}_1$ and dash-dot red lines for $\mathscr{C}_2$. The superposition of three regimes for two cells creates at most nine pairs of regimes $(O_1;O_2)$ which are captioned between brackets and whose operating regions are differently coloured. We note with a yellow star the intersection point between the lower bounds of $\mathscr{R}_1^*$ and $\mathscr{R}_2^*$. This intersection point refers to $\Gamma^* = (\gamma_1^*;\gamma_2^*)$; O^* is the pair of regimes whose region contains Γ^*.

Γ^* is the optimal solution we are looking for. Indeed, this point is inside both $\mathscr{R}_1^*$ and $\mathscr{R}_2^*$, then both cells meet their rate constraints. This point is also on the lower bounds of $\mathscr{R}_1^*$ and $\mathscr{R}_2^*$: rate constraints are then met with the minimal power budget. It remains to prove that the purple and blue lower bounds of $\mathscr{R}_1^*$ and $\mathscr{R}_2^*$ will always cross themselves. The geometrical reasoning below lets to prove it:

Step 1. Define two continue functions φ_1 and φ_2 represented respectively by $(\mathscr{D}_1^k)_k$ in purple and $(\mathscr{D}_2^k)_k$ in blue.

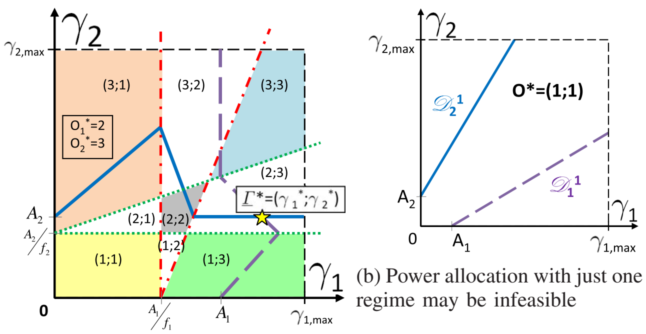

(a) Optimal Γ^* and regimes pair O^*

(b) Power allocation with just one regime may be infeasible

Fig. 3: Numerical results for two given scenarios $\mathscr{P}_S$

Step 2. By a continue transformation ψ of the map applied to φ_1, the graphic representation of $\bar{\varphi}_1 = \psi \circ \varphi_1$ becomes the straight vertical line $\gamma_1 = A_1$.
Step 3. $\bar{\varphi}_1$ is continue as composition of continue functions.
Step 4. Two straight non parallel lines are always secant.
Step 5. $\bar{\varphi}_1$ and φ_2 are then secant at a point Γ^0.
Step 6. The image of an intersection under a continue function remains an intersection.
Step 7. By the inverse continue transformation ψ^{-1} applied to Γ^0, φ_1 and φ_2 are secant at point $\Gamma^* = \psi^{-1}\left(\Gamma^0\right)$.
Some details: transformation ψ at **Step 2** is something like a homothetic transformation or a dilation of the map, and **Step 5** is corroborated by the intermediate value theorem.

VI. Numerical Results

In this section we give numerical results for our algorithm. Our poor assumptions may be verified by many cellular networks with in-band interference. However, NC requests channel estimations hardly achievable in case of highly variable communication contexts. Thus, our approach fits especially to systems with low fading variations and low users mobility: a power budget is allocated to neighbour cells while adaptive channel aware techniques can deal with fast variations.

Most previous works propose power allocation algorithms where interference is always processed as noise [17]–[19]. But such approaches fail as soon as noisy regime assumption is not consistent any more with the momentary communication context. Figure 3b illustrates one particular scenario where rate constraints cannot be met by a one-level interference classifier adopting just the noisy regime. Achievable SNR regions $\mathscr{R}_1^*$ and $\mathscr{R}_2^*$ are just limited by a single bound, respectively $\mathscr{D}_1^1$ and $\mathscr{D}_2^1$, which never cross, even ad infinitum. In these conditions, both sources cannot transmit simultaneously on the same band; either time and/or frequency sharing should be performed, or a user must be rejected (*i.e.,* no transmission). Section V proved that adapting interference strategy to the perceived interference leads always to a solution.

$\mathscr{P}_S = \{\mathbf{R_1}; \mathbf{R_2}; f_1; f_2\}$ fully states the problem. $\mathbf{R_i}$ is actually the target spectral efficiency in bit per channel use (BPCU), while f_i emulates simultaneously several scenarios of interference: numerous channel coefficients pairs $(g_{i,i}; g_{i,j})$ stand for the same f_i. Changing one of four parameters in $\mathscr{P}_S$ leads to another optimal solution. $\mathscr{P}_S = (2;4;5;7)$ defines for instance an interference limited scenario (*i.e.,* deep fading, border cell user, etc.), since both f_i are greater than one. In this case, optimal solution is given on Figure 4a: (γ_1^*, γ_2^*) should equal Γ^*, while $\mathscr{C}_1$ and $\mathscr{C}_2$ should process interference with techniques designed respectively for "interference cancellation" and "joint decoding" regimes ($O^* = (3;2)$).

To compute optimal power vector P^*, we assume hereafter a system of two femtocells where d_i experiences $-105dBm$ of thermal noise, fading coefficient $h_{i,i}$ and path loss attenuation

$$L_i^{dB} = 37 + 30 \cdot \log_{10}(d^{(i)}),\ d^{(i)} = dist(s_i; d_i)\ [m]. \quad (13)$$

We also consider, for instance, the parameters $d^{(1)} = 25m$, $d^{(2)} = 30m$, $h_{1,1} = 0.1$ and $h_{2,2} = 0.05$. Then P^* can be computed based on (14) where overall channel gain $g_{i,i}$ is expressed with path loss and fading attenuations. Γ^* and (14) lead to $P_1^* = 0.74mW$ and $P_2^* = 82mW$: both powers are lower than the conventional limitation $\mathbf{P_{max}} = 200mW$ for femtocells power budget.

$$P_i^* = \frac{N_0}{g_{i,i}} \cdot \gamma_i = \frac{N_0 \cdot 10^{\frac{L_i^{dB}}{10}}}{|h_{i,i}|^2} \cdot \gamma_i \quad (14)$$

A surprising scenario is shown on Figure 4b where $\mathscr{P}_S = (2;2;1.75;1.75)$: three solutions are feasible. It was proved in Section V that at least one solution always exists. Further reasoning would show that each scenario $\mathscr{P}_S$ admits at most three solutions with non-zero probability. Such a result is not at all a limitation: optimal vector P^* can be selected by a metric, for instance the sum-power minimization $(P_1^* + P_2^*)$.

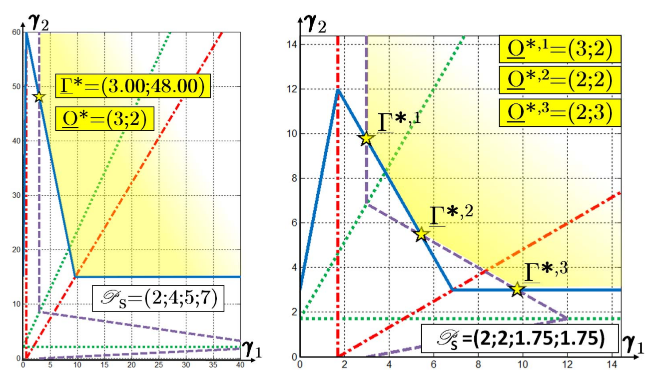

(a) Strong interference

(b) Three optimal solutions

Fig. 4: Numerical results for two given scenarios $\mathscr{P}_S$

Finally, we compare by numerical simulations our adaptive algorithm to a power allocation with just a noisy regime; our evaluation context is a system of two interference-limited and mobile femtocells. d_i randomly moves in $\mathscr{C}_i$ of radius $20m$, while s_1 and s_2 are located at most $100m$ apart. Destinations experience path loss attenuation (13), log-normal shadowing with $8dB$ standard deviation, $-105dBm$ of noise and Rayleigh fading. $\mathbf{R_i}$ is randomly selected in the transmission rate set $\underline{\mathbf{R}} = \{1;2;4;6;8\}$. If at least one optimal power P_i^* exceeds $\mathbf{P_{max}}$, then minimal power $P_{TS,i}^*$ is assigned by a Time Sharing (TS) process. $P_{TS,i}^*$ is defined such that each source s_i uses alone the shared frequency band half the time, as specified in Equation (15). If $P^*_{TS,i}$ still exceeds $\mathbf{P_{max}}$, then both transmissions are rejected: $P^* = (0;0)$.

$$R_i \leq \frac{1}{2} \cdot \log_2 \left(1 + \frac{g_{i,i} \cdot P_{TS,i}}{N_0}\right) \tag{15}$$

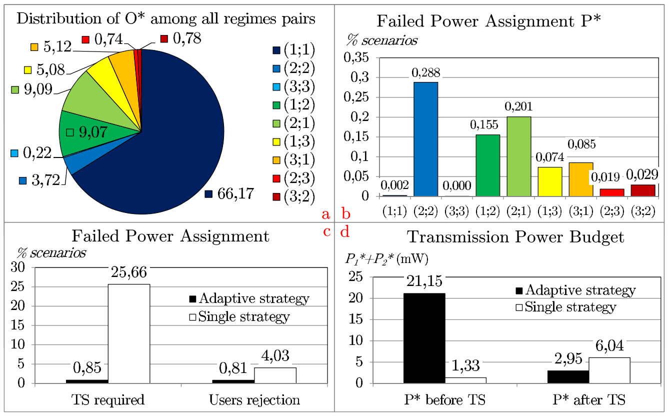

Fig. 5: Adaptive vs. Single-scheme Power Allocation

Simulation results are obtained across 10^7 random scenarios and are shown on Figures 5a–5d. Fig.5a illustrates the distribution of O^* among all pairs and proves the relevance of our interference classification, since $O = (1;1)$ cannot be used for all scenarios. Fig.5b and 5c show the frequency of failed power assignments: we plot first the failure "$P^* > \mathbf{P_{max}}$" (Fig.5b and Fig.5c-left) and then the users rejection "$P^*_{TS} > \mathbf{P_{max}}$" (Fig.5c-right). Black and white bars describe respectively performance of the adaptive algorithm and the single noisy strategy.

Fig.5d plots on left-side the initial and on the right the final (after user rejection) average power budgets. Before users rejection, the single-strategy seems to be more power-efficient than our approach, but this appearance is deceptive. Indeed, a single-strategy can compute negative P^* (Fig.3b): on the 25.66% of initial failed power assignments, 25.63% are due to $P^* < 0$ and just 0.03% to $P^* > P_{max}$. Negative P^* cannot be taken into account on Fig.5d: the comparison is then unfair, since worse scenarios are counted for our approach but rejected for the single-strategy. In effect, a quarter of transmissions are infeasible with the single-strategy, while less than 1% of transmissions are too power-greedy with our algorithm. Furthermore, we note that with our approach just 0.04% of failed power assignments are solved by TS (Fig.5c, 0.85% before TS to 0.81% after TS), whereas the power budget is reduced in the same time of 86% with users rejection (Fig.5d, $21.15W$ before TS to $2.95W$ after TS). In case of the single-strategy, 21% of failed scenarios (*i.e.,* negative and excessive P^*) are solved by TS; but ultimately power budget and users rejection are respectively 51% and 80% greater than the ones achieved with our algorithm.

VII. Conclusion

This paper proposes a centralized algorithm for power allocation in interference limited cellular networks where cells target to meet QoS constraints. Our approach is based on a classification of interference perceived in each cell: interference is not always a problem if efficient schemes deal with it. Both theoretical and numerical results illustrate three major achievements for our algorithm. First, QoS constraints of each cell are jointly met. Second, the computed transmission power is minimized for avoiding energy waste. Third, interference mitigation strategies are adaptively selected according to the momentary communication context so as to efficiently cope with the perceived interference. Numerical results prove that our approach notably outperforms a power allocation with a single noisy strategy, both in terms of users rejection and power budget minimization. Future works will focus on the distribution of the algorithm and extend results to networks with more than two neighbour cells.

References

[1] Y. Xiang, J. Luo and C. Hartmann, "Inter-cell interference mitigation through flexible resource reuse in OFDMA based communication networks," *Proc. EW 2007*, pp. 1–7, Apr. 2007.

[2] D. Tse and P. Viswanath, "Fundamentals of wireless communication," Cambridge University Press, May 2005.

[3] J. Boutros, N. Gresset, L. Brunel and M. Fossorier, "Soft-input soft-output lattice sphere decoder for linear channels," *IEEE GLOBECOM 2003*, pp. 1583–1587, Dec. 2003.

[4] K. Gomadam, V.R. Cadambe and S.A. Jafar, "Approaching the capacity of wireless networks through distributed interference alignment," *IEEE GLOBECOM 2008*, pp. 1–6, Nov. 2008.

[5] S.A. Jafar, "Exploiting channel correlations - Simple interference alignment schemes with no CSIT," *submitted to arXiv*, Oct. 2009, downloadable at http://arxiv.org/abs/0910.0555.

[6] S.M. Perlaza, M. Debbah, S. Lasaulce and J.-M. Chaufray, "Opportunistic interference alignment in MIMO interference channels," *IEEE PIMRC 2008*, pp. 1–5, Sep. 2008.

[7] A.J. Goldsmith and S.-G. Chua, "Adaptive coded modulation for fading channels," *IEEE Trans. Comm.*, vol. 46, no. 5, pp. 595–602, May 1998.

[8] S. Boyd and L. Vandenberghe, "Convex optimization," *Cambridge University Press*, 2006.

[9] M. Chiang, C.W. Tan, D.P. Palomar, D. O'Neill and D. Julian, "Power control by geometric programming," *IEEE Trans. Wireless Comm.*, vol. WC-6, no. 7, pp. 2640-2651, Jul. 2007.

[10] T. Cover and J. Thomas, "Elements of Information Theory," *Wiley*, 2006.

[11] R.H. Etkin, D.N.C. Tse and H. Wang, "Gaussian interference channel capacity to within one bit," *IEEE Trans. Info. Theory*, vol. IT-54, no. 12, pp. 5534–5562, Dec. 2008.

[12] S.A. Jafar and S. Vishwanath, "Generalized degrees of freedom of the symmetric Gaussian K user interference channel," *submitted to arXiv*, Apr. 2008, downloadable at http://arxiv.org/abs/0804.4489.

[13] T.S. Han and K. Kobayashi, "A new achievable rate region for the interference channel," *IEEE Trans. Info. Theory*, vol. IT-27, no. 1, pp. 49–60, Jan. 1981.

[14] T.M. Cover, A. El Gamal and M. Salehi, "Multiple access channel with arbitrarily correlated sources," *IEEE Trans. Info. Theory*, vol. IT-26, no. 6, pp. 648–657, Nov. 1980.

[15] A.S. Motahari and A.K. Khandani, "Capacity bounds for the Gaussian interference channel," *IEEE Trans. Info. Theory*, vol. IT-55, no. 2, pp. 620–643, Feb. 2009.

[16] A.B. Carleial, "A case where interference does not reduce capacity (Corresp.)," *IEEE Trans. Info. Theory*, vol. IT-21, no. 5, pp. 569–570, Sep. 1975.

[17] S. Kandukuri and S. Boyd, "Optimal power control in interference-limited fading wireless channels with outage-probability specifications," *IEEE Trans. Wireless Comm.*, vol. WC-1, no. 1, pp.46–55, Jan. 2002.

[18] C.-H. Yih and E. Geranotis, "Centralized power allocation algorithms for OFDM cellular networks," *IEEE MILCOM 2003*, pp. 1250–1255, Oct. 2003.

[19] A. Gjendemsjo, D. Gesbert, G.E. Oein and S.G. Kiani, "Optimal power allocation and scheduling for two-cell capacity maximization," *WiOPT 2006*, vol. 95, no. 12, pp. 1–6, Apr. 2006.